JOM, Vol. 72, No. 9, 2020
https://doi.org/10.1007/s11837-020-04258-6

Metal Powder Recyclability in Binder Jet Additive Manufacturing

SAEREH MIRZABABAEI,[1,2] BRIAN K. PAUL,[1,2] and SOMAYEH PASEBANI [1,2,3]

1.—School of Mechanical, Industrial and Manufacturing Engineering, Oregon State University, Corvallis, OR 97330, USA. 2.—Advanced Technology and Manufacturing Institute (ATAMI), Corvallis, OR 97330, USA. 3.—e-mail: somayeh.pasebani@oregonstate.edu

The recyclability of 316L stainless steel powder in the binder jetting process has been determined. The powder characterization results demonstrated a 22% increase in the number of coarse particles (> 30 μm) and an 18.2% reduction in the number of small particles (< 10 μm) after recycling up to 16 times. A few elongated and irregular-shaped particles were found after recycling, possibly due to particle agglomeration during handling and sieving. A negligible increase in the oxygen content by 0.036% was detected in the recycled powder. The density of sintered parts produced using recycled powder was approximately 1.5% lower than when using fresh powder due to the changes in the particle size distribution and the flowability of the powder caused by the changes in morphology. Final parts built using fresh and recycled powder showed similar hardness (155 ± 3 HV and 165 ± 9 HV) and yield strength (206 ± 16 MPa and 192 ± 10 MPa), respectively.

INTRODUCTION

Metal additive manufacturing (AM) is rapidly evolving from rapid prototyping into manufacturing of end-use products in various high-value sectors. AM enables the production of complex geometries in one step without the need for expensive tooling. Despite the revolutionary development of metal AM, its environmental effects have not been studied extensively. In powder bed processes, a considerable amount of metal powder is required to operate the machine, while only a small portion of it is used to build parts. The cost of powder for powder-based AM processes can range from 10% to 50% of the manufactured part cost for most alloys.[1] Therefore, one cost-effective and environmentally driven approach to reducing powder consumption is powder recycling, thus enabling reuse of the same powder for multiple consecutive AM builds. The effect of the metal powder condition after recycling on the properties of the final part must be investigated to determine whether powder quality protocols are required.

The characteristics of the powder determine the final density, mechanical properties, and performance of the additively manufactured parts.[2] These include the morphology, chemistry, particle size distribution (PSD), powder bed density, flowability, and spreadability. The powder manufacturing process determines the powder characteristics.[1] Atomization is the most popular manufacturing process for powder for use in additive manufacturing and powder metallurgy.[3] While water-atomized metallic powders are more common and cost effective in traditional press and sintering techniques, gas-atomized powders have lower oxygen content, spherical shape, and better flowability. As a result, gas-atomized powders are more commonly used in metal injection molding (MIM) and additive manufacturing processes.[4–6]

The powder morphology and particle size distribution influence the powder flowability, spreadability, and powder bed density.[4] Small particles tend to agglomerate and show poor flowability due to high interparticle friction, impeding dense packing.[7] The porosity size and distribution in powder metallurgy (P/M) compacts are influenced by the initial particle size.[8] However, the shape of the particles significantly affects the packing density. Coarser particles may result in better packing density than fine particles with similar (broad/narrow) PSD and similar sphericity due to lessened interparticle friction.[9] Furthermore, the use of large particles tends to increase the surface roughness of the part.[10] It has been reported that spherical particles with narrow PSD can show improved flowability as

(Published online July 6, 2020)

well as powder bed density.[4] Therefore, in any powder-based AM technology, determination of the optimal PSD is crucial, as the part density and quality are significantly affected by the powder characteristics.[11,12]

Several efforts have been made to address powder recyclability within powder bed fusion (PBF) technologies such as selective laser melting (SLM)[2,13–15] and electron beam melting (EBM).[15,16] Ardila et al.[2] studied the impact of reuse of gas-atomized Inconel 718 powder in the SLM process on the powder characteristics and mechanical properties of manufactured parts, finding no significant change in the powder quality or the properties of test parts after recycling 14 times.

Jacob et al.[17] reported on the powder quality and the properties of test specimens after recycling gas-atomized 17-4PH powder 11 times in a laser-based PBF (LPBF) process. Powder characterization revealed no significant change in the shape, morphology, or size of the particles. The mechanical properties of the parts manufactured from recycled powder were equivalent to those manufactured from fresh powder. Nandwana et al.[16] used Inconel 718 and Ti-6Al-4V powders in the EBM process and investigated the changes in the powder properties after recycling six and five times, respectively. No noticeable changes were observed in the flowability, morphology, or size distribution of the Inconel 718 and Ti-6Al-4V powders as a function of the number of build cycles. However, it was revealed that, after recycling several times, Ti-6Al-4V powder was prone to pick up oxygen during the powder changing step as well as during part recovery in the powder recovery system, while Inconel 718 powder was found to be more chemically stable.

Furthermore, some studies have claimed that the mechanical properties are slightly affected by the properties of the recycled powder. O'Leary et al.[13] investigated the recycling of Ti-6Al-4V powder in SLM. The number of fine particles was reduced after recycling five times, while the number of coarse particles increased, leading to a higher overall particle diameter. A reduction in the sphericity of the powder particles was also observed. Additionally, chemical composition analysis of the (fresh and recycled) powders and the manufactured parts revealed no significant trend in the change of the oxygen content of the powder after recycling. Overall, the oxygen content of components produced from either fresh or recycled powder was higher than that of powders, due to the absorption of oxygen into the laser-melted parts during the SLM process. The level of absorbed oxygen in all parts produced from grade 23 ELI Ti-6Al-4V powder (fresh and recycled) was close to the acceptable limit of oxygen (0.2 wt.%) for grade 5 Ti-6Al-4V.

Seyda et al.[14] studied the effect of recycling gas-atomized Ti-6Al-4V powder in SLM on the powder characteristics and mechanical properties of parts. After recycling the powder 12 times, the fraction of coarse particles increased. Furthermore, recycled powder demonstrated higher apparent density and better flowability, as revealed by measurements of the angle of repose. This was due to their comparably low number of fine particles, which reduced interparticle friction forces, hence improving the flowability. Parts manufactured from recycled powder showed slightly higher density and better mechanical properties. Strondl et al.[15] characterized fresh and recycled Ti-6Al-4V and Ni powder for EBM and SLM, respectively. The recycled powder for the EBM process was treated by blasting followed by the standard procedure recommended by the EBM equipment manufacturer, while the recycled powder for the SLM process was only sieved with a 63 μm mesh screen. After recycling, the SLM powder showed better flowability and a coarser particle size distribution due to the loss of finer particles. However, the flowability of the recycled EBM powder was worse than that of the fresh powder due to the greater number of finer particles, likely resulting from the treatment of the powder by blasting, which caused removal of satellites and broke the bonds between particles. Furthermore, blasting left mechanical impact marks on the surface of the recycled EBM powder particles, which reduced their sphericity. Mechanical testing revealed that the tensile strength was not affected by the changes in the powder properties, while the impact toughness decreased by about 16% for parts manufactured by SLM using the recycled powder.

To date, regardless of the current ASTM F3049 standard (for characterizing metal powder properties for AM systems), there are no published standards describing best practices to maintain specific characteristics during powder recycling. However, controlling the powder characteristics in metal AM processes is required to produce high-fidelity parts with reliable properties. It is thus critical to consider the variations and inconsistencies that occur during different powder manufacturing processes (e.g., atomization), AM processes, process parameters, materials studied, recycling strategies, and number of recycles to establish an effective universal recycling procedure.

Recycling of powder in binder jetting (BJT) processes has neither been studied nor published elsewhere. This may be in part because the BJT process does not rely on thermal fusion, which is the main mechanism increasing the particle size in LPBF. However, BJT processes are prone to splashing of ink (binder), which can potentially enhance agglomeration and binding of particles.[18,19] Figure 1 shows a micrograph of BJT-processed powder collected from the vicinity of built parts after finishing the BJT process. Significant agglomeration is observed due to excessive binder splash and binder migration out of the bounding box. The presence of these agglomerated particles adversely affects the PSD.

Furthermore, the depowdering strategy (a part of the BTJ process and recycling steps) may alter the powder morphology. Any resulting changes in the powder size and morphology could change the densification behavior and mechanical performance. While BJT is generally recognized to have good powder recyclability, verification of this assertion is crucial to enable further scalability of this process. The present work focuses on evaluating the recyclability of 316L stainless steel (SS) powder up to 16 times in the BJT process, by characterizing the properties of the powder and quality of the final part.

EXPERIMENTAL PROCEDURES

Gas-atomized 316L stainless steel (SS) powder (D_{90} = 22 μm) with the chemical composition presented in Table I was procured from Hoeganaes. Fresh 316L powder was loaded into a laboratory-scale metal binder-jet tool, and cubes with dimensions of 10 mm × 10 mm × 10 mm and tensile bars (according to ASTM E8) were manufactured for metallurgical and mechanical analysis, respectively. Each batch of as-printed samples was cured at 150°C for 3 h and sintered inside a tube furnace (1630-20HT; CM furnaces Inc.) filled with 96% Ar-4% H_2 atmosphere with the following heating profile: heating at 7°C/min from room temperature (RT) to 400°C, holding at 400°C for 5 h (for debinding), then 7°C/min to 800°C, and 3°C/min to 1380°C, holding at 1380°C for 2 h, then cooling at 3°C/min to 800°C and finally at 7°C/min to RT in the furnace.

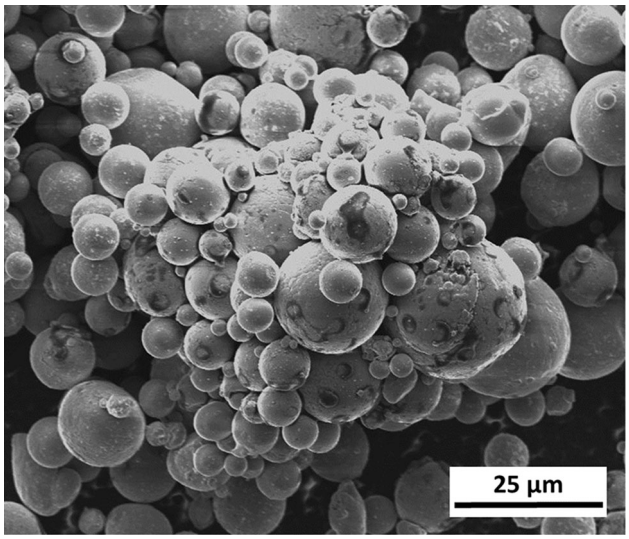

Fig. 1. SEM micrograph of powder agglomerates in BJT-processed SS 316L powder due to the presence of binder residues (powder sample collected from vicinity of built parts after BJT printing).

To produce identical parts, a specific recycling strategy was adopted, in which all the powder within a specific build was recycled the same number of times. In this strategy, one cycle consists of multiple build jobs using powder in the same condition, meaning the initial powder batch was allocated to as many build runs as possible. Then, the whole batch of used powder (after recycling) underwent another build cycle. These powder reuse cycles were repeated until another build job was not possible (due to an insufficient amount of powder for another build job). In other words, in batch number 16, all the powder had been recycled 16 times. This favorable strategy involves collective degradation of powder but few powder variations in one batch.[21] After each build job, the powder remaining in the build plate was collected, dried at 180°C overnight in vacuum to remove adsorbed moisture possibly from environment and water-based binder, followed by 325 mesh (− 45 μm) sieving to recycle. This process was repeated 16 times, and the recycled powder was reused in 16 build cycles.

The tap density (TD) and apparent density (AD) of fresh and recycled powder were measured (three times) according to ASTM B527-15 and ASTM B212-17, respectively, to indicate the flowability of the powders using the Hausner ratio (AD/TD). Particle size distribution (PSD) analysis was performed using a laser diffraction-based particle analyzer (Malvern Mastersizer 3000). Powder morphology and elemental composition analyses were conducted using an FEI Quanta 600 scanning electron microscope (SEM) equipped with energy-dispersive x-ray spectroscopy (EDS). The oxygen and carbon content of the fresh and recycled powders were analyzed using LECO ON736 and C744 analyzers, respectively.

The green density of the as-printed parts (cubes) was calculated based on their volume and mass. The final density of the sintered parts was measured according to the Archimedes method.

Table I. Chemical composition of stainless steel 316L powder

	Elemental content, wt.%										
Alloy	**C**	**Mn**	**Cr**	**Si**	**Ni**	**Mo**	**S**	**O**	**N**	**P**	**Fe**
SS 316L powder	0.018	1.64	17.7	0.73	12.6	2.67	0.007	0.09	0.08	–	Balance
SS 316L (ASTM F3184)[20]	0.030	2.00	16.0–18.0	1.00	10.0–14.0	2.00–3.00	0.030	–	–	0.045	Balance

Microstructural characterization of parts manufactured from fresh and recycled powder was conducted by optical microscopy (Zeiss, Axiotron) and SEM. The hardness of the built parts was measured using a LECO microhardness tester (LM-248AT). Tensile testing was performed on an Instron 5969 at ambient temperature and strain rate of 10^{-4} s^{-1}.

RESULTS AND DISCUSSION

Powder Characterization

The flowability of the fresh and recycled powder was evaluated via the Hausner ratio, which provides a measure of the friction condition in a moving powder mass,[22] as shown in Fig. 2. A Hausner ratio above 1.25 indicates relatively poor powder flowability.[4] The fresh powder had a Hausner ratio of 1.13, indicating good flowability. Recycled powder showed similar flowability but slightly lower AD and TD. Fresh powder exhibited highly consistent behavior with a small standard error on AD and TD. The SEM micrographs of fresh powder were almost all similar and consistent with Fig. 2a. However, as reported for recycled powder, there were relatively greater variations in the AD and TD measurements. Although the recycled powder consisted of some irregular-shaped particles, as shown in Fig. 2b, the amount of these particles was not very high, thus they did not necessarily appear in all of the SEM micrographs, suggesting that different samples of recycled powder may or may not contain irregular particles.

Figure 2 shows the morphology of the fresh and recycled SS 316L powder used as feedstock for the BJT process. The fresh powder particles (Fig. 2a) were spherical and well defined, while the recycled powder (Fig. 2b) showed larger particles and slightly elongated irregular-shaped particles. After recycling 16 times, particle agglomeration was still negligible.

The BJT-processed powder demonstrated massive powder agglomerates (> 50 μm) due to binder splash,[19] as shown in Fig. 1. The extent of undesired binder penetration can be controlled by binder saturation adjustment; however, binder spreading is a complicated process that depends on many factors, including the particle size and particle packing.[23] BJT-processed powder demonstrated $D_{90} > 100$ μm, with most of the larger particles (> 50 μm) being powder agglomerates with binder residue on the surface of particles. The presence of these agglomerates in the recycled powder batch could negatively affect the powder spreading in the bed. Sieving (-45 μm) was used to prevent massive agglomerated particles from entering the recycled powder batches. Thus, the fraction of agglomerates in the powder recycled 16 times was kept low.

the particle size distribution affects the powder flowability and its spreadability in the bed, and thereby the final density of the green part.[11,13] Figure 3 shows that the powder particle distribution was shifted to the right, indicating coarser sizes with larger D_{10}, D_{50}, and D_{90} values after recycling 16 times. Furthermore, the number of fine particles (< 10 μm) was significantly reduced from $37.16 \pm 0.33\%$ in the fresh powder to $18.92 \pm 0.65\%$ in the recycled powder (volume density). A large amount of fine particles results in

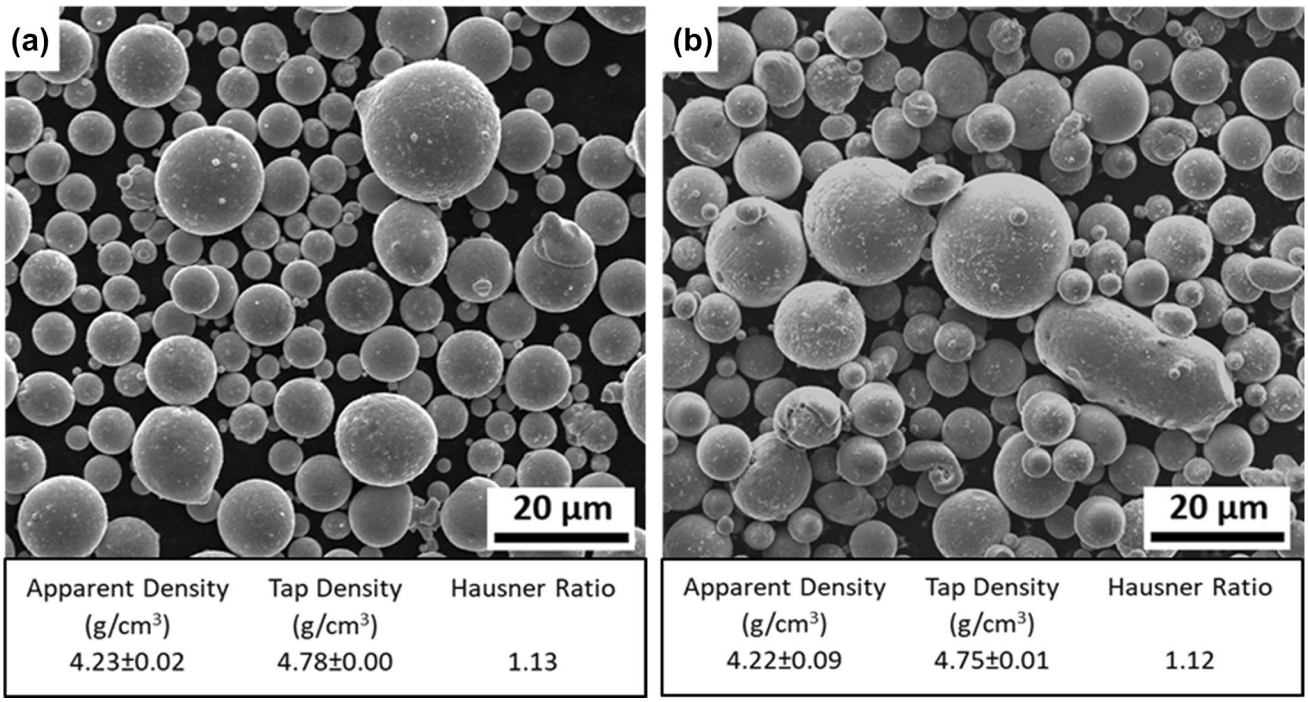

Fig. 2. SEM micrographs of 316L stainless steel: (a) fresh powder, and (b) recycled powder after 16 builds.

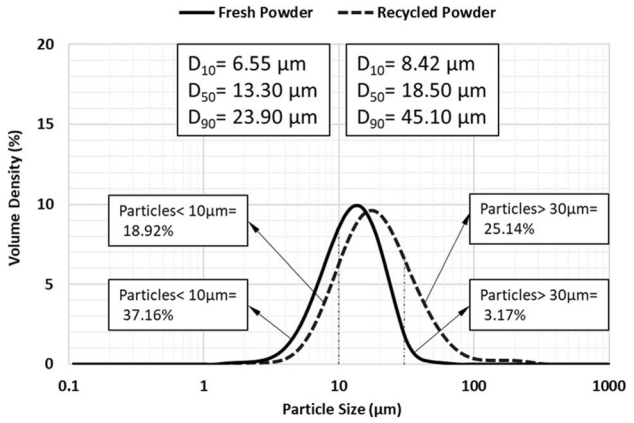

Fig. 3. Particle size distribution for SS 316L obtained by laser diffraction technique: fresh powder and after recycling 16 times.

poor flowability due to strong adhesive forces and interparticle friction,[24] while a larger median particle size improves the flowability of the powder.[25] Therefore, the coarser PSD and the loss of fine particles in the recycled powder led to slightly better flowability. The mean particle size of the fresh and recycled powder was 13.30 ± 0.57 μm and 18.50 ± 0.49 μm, respectively.

After each cycle of BJT, the unused powder was collected to be recycled. The collected powder consisted of two fractions: the print bed portion and the depowdering fraction. In the main fraction, which was collected from the print bed, particles lying outside of the boundaries of the part were not exposed to binder droplets and did not show agglomerates, while other particles in regions adjoining the boundaries of the part exhibited significant agglomeration and the presence of residual binder (Fig. 1). A high fraction of the finer particles could be lost during collection and handling. The second portion of unused powder was then collected during the depowdering of the green BJT parts. Depowdering of green parts was performed using special soft brushes, followed by pressurized air. Hence, the fine particles were dusted off, and the sphericity of the remaining larger particles was reduced slightly due to the applied pressure. However, the amount of powder collected during de-powdering was low compared with that collected from the bed, leading to the presence of a low fraction of elongated irregular particles in the recycled powder. Depowdering using pressurized air might alter the dimensional accuracy of the part. The entire batch of new powder contained a limited number of elongated particles. The fraction of such irregular particles accumulated in each batch of powder after repeated recycling, with a loss of finer particles.

All the collected powder was then heated overnight and then sieved. A significant fraction of finer particles was lost to the air during sieving, leading to a coarsening of the PSD. Additionally, despite sieving the powder, some agglomerated particles (total size < 45 μm) that may have formed due to the presence of residual binder were found in the recycled powder, further contributing to the particle size coarsening. Typically, metal powders with mean particle size < 20 μm have high potential to achieve full density in BJT[26]; hence, the recycling strategy applied in this study is not direct detrimental in terms of densification.

Chemical Composition of Powders

Potential sources of contamination during powder recycling in BJT include oxygen pick-up, residual polymeric binder, moisture pick-up (from the environment as well as water-based binder), and other contaminants present in the working atmosphere that could alter the chemical composition of the powder after recycling. Fresh and recycled powders were analyzed for their oxygen and carbon content. The elemental analysis revealed that the carbon content of the fresh and recycled powders remained consistent at $0.0152 \pm 0.0001\%$ and $0.0154 \pm 0.0001\%$, respectively. Meanwhile, the amount of oxygen was slightly higher for the recycled powder ($0.1194 \pm 0.0013\%$) than the fresh powder ($0.0835 \pm 0.0004\%$). It is expected that the recycled powder likely picked up additional oxygen due to the increased amount of handling and sieving (which was not done inside a glove box). It is noteworthy that, according to ASTM F3184, SS316L powder has no oxygen content. However, the as-received powder contained about 0.09% oxygen, as reported by the manufacturer (Table I) and as analyzed in this study.

During sintering, the residual oxygen content of SS 316L tends to react with alloying elements and form oxides in the sintered parts, and the presence of oxides may impede densification during sintering.[27] Powders with lower oxygen content have better sinterability and result in higher densification.[28] During sintering of 316L, oxides containing Mn and Si are more likely to be formed due to the lower ΔG (Gibbs free energy) of their oxidation reactions. Moreover, the formation of SiO_2 and MnO reduces the amount of Si and Mn elements, which are essential contributors to the strengthening of the alloy,[29] thus leading to inferior tensile and ductility properties.[27] The formation of Si and Mn oxides during the LPBF process could enhance the mechanical properties[30] but may have detrimental effects on the densification of the sintered parts. Varying amounts of oxides may be present in the BJT parts, depending on the oxygen content. However, in this study no particular oxides were detected in the BJT-manufactured parts by EDS analysis. Despite the possible negative impacts of the oxygen content of the powder on the density and mechanical properties of the final parts, the oxygen increase after recycling seemed to be insignificant compared with that in the fresh powder and could

be attributed to the drying step between each recycling.

Part Density and Shrinkage

The green and final density of the specimens manufactured from fresh powder were higher than for those obtained using the recycled powder (Fig. 4a). The observed variations in the green and final density of the parts produced from the fresh and recycled powder can be explained by the morphological differences. Powder with a lower amount of small particles displays less capacity to fill interstices between larger particles, hence less packing density, less green density, and lower final density.[7] The lower green and final density of the parts manufactured by BJT from recycled powder support the latter statement. In other words, the lower densification of the recycled powder can be justified by its coarser PSD.[31] Liu et al.[32] investigated the effect of the powder properties in SLM processes, concluding that powder with a broader range of particle size resulted in a higher powder bed density and generated parts with a higher final density of 99.30%, while powder with a narrower

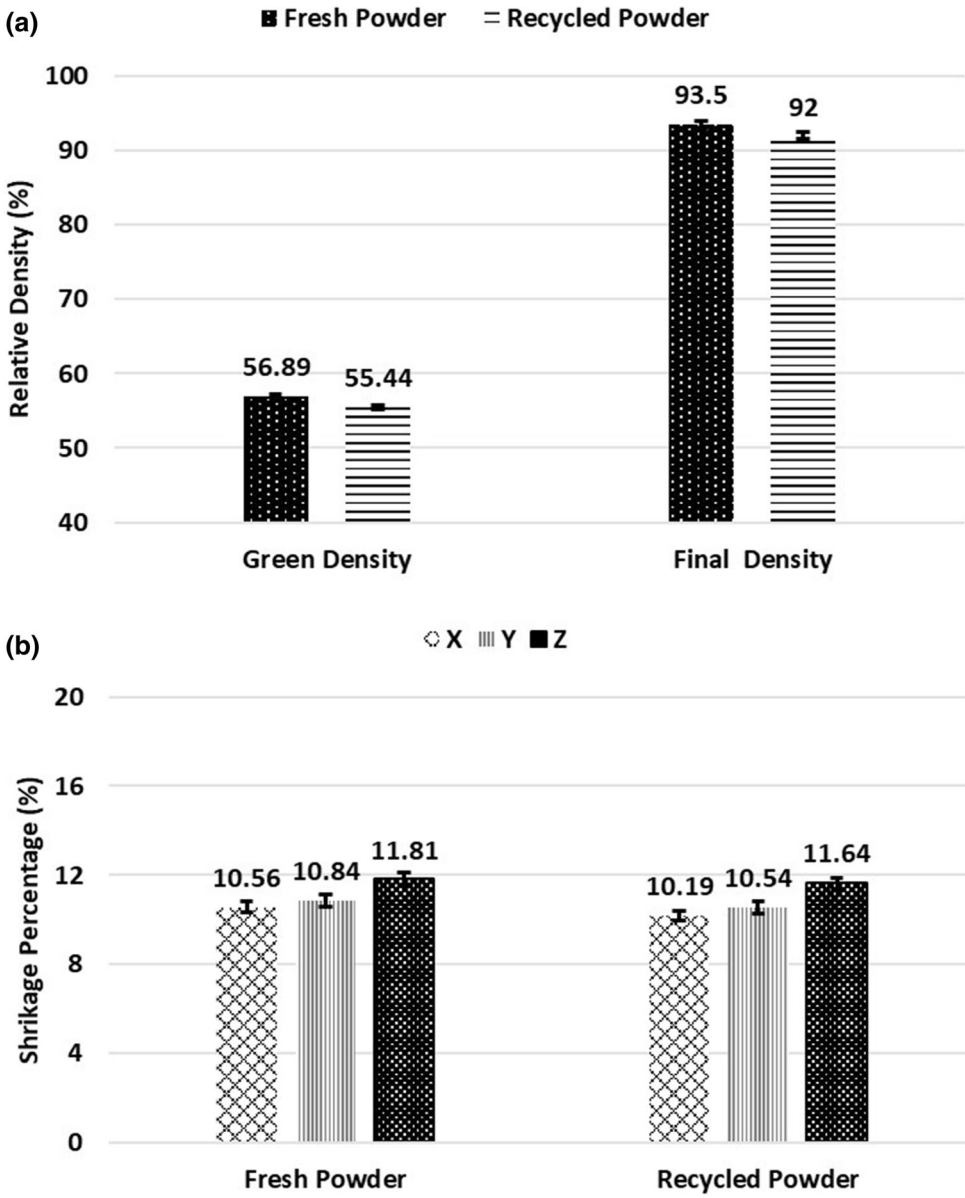

Fig. 4. (a) Green and final relative density of parts manufactured by BJT from fresh and recycled SS 316L powder, (b) degree of shrinkage after sintering for specimens made from fresh and recycled SS 316L powder.

PSD resulted in a final density of only 97.22%. Therefore, the lower green and final density of the manufactured part by BJT from the recycled powder can be attributed to the coarser PSD due to the fewer fine particles in the recycled powder.

The degree of shrinkage of the parts manufactured by BJT using the fresh and recycled powder is shown in Fig. 4b. The shrinkage when using the fresh powder was 10.56 ± 0.23%, 10.84 ± 0.28%, and 11.81 ± 0.31% in the *X*-, *Y*-, and *Z*-direction, respectively. Meanwhile, the shrinkage when using the recycled powder was 10.19 ± 0.21%, 10.54 ± 0.26%, and 11.64 ± 0.25% in in *X*-, *Y*-, and *Z*-direction, respectively.

The typical shrinkage range reported for BJT-manufactured parts is up to 20%.[33] In Fig. 4b, the *X* and *Y* directions are on the build plate. Therefore, Fig. 4b shows that the shrinkage in the build direction (*Z*-direction) was the highest for the samples obtained using both the fresh and recycled samples, indicating greater interlayer (parallel to the build direction) porosity rather than within layers (transverse and perpendicular to the build direction).

The porosity distribution in the parts manufactured by BJT using the fresh and recycled powders is presented in Fig. 5. ImageJ software was used to analyze and measure the pore size in the samples. Parts produced from the fresh powder showed relatively round and smaller pores with average size of 4.18 ± 1.10 μm, whereas parts produced from recycled powder displayed larger pores with various shapes, including round and irregular-shaped pores with average size of 5.83 ± 1.52 μm. The average particle size and PSD influence the pore size and distribution in the powder bed.[34] Fine particles result in a high fraction of small pores distributed throughout the entire sample, while coarse particles produce a small number of larger pores, randomly distributed in the sample.[8]

The fresh powder consisted of fully spherical particles with smaller size (D_{10} = 6.55 μm and D_{90} = 23.90 μm) that resulted in smaller and near-round-shaped pores. In contrast, recycled powder exhibited larger particle size (D_{10} = 8.42 μm and D_{90} = 45.10 μm) with fewer fine particles that resulted in an additional 1.5% larger irregular-shaped porosity. Similarly, Spierings et al.[10] investigated the effect of the PSD on the density of SLM parts and concluded that an increase of the particle size from D_{10} = 6.3 μm and D_{90} = 30.79 μm to D_{10} = 15.64 μm and D_{90} = 59.69 μm increased the part porosity by approximately 0.5%.

Microstructure of BJT-Manufactured Parts After Recycling

The microstructure of the parts manufactured by BJT using fresh and recycled powder is shown in Fig. 6a and b, respectively. In both samples, pores were located along grain boundaries and in grain interiors. This was expected, because none of the samples reached full density. Samples produced using fresh powder had porosity of 6.5 ± 0.4% with relatively small and medium-sized round pores and some irregular pores, as shown in Fig. 6a. However, samples produced from recycled powder demonstrated a higher level of porosity of 8.0 ± 0.5% with a greater amount of large-sized and irregular-shaped pores, as shown in Fig. 6b. Both samples were sintered in Ar and showed a microstructure with channels of pores along the grain boundaries that would decelerate grain boundary diffusion. The

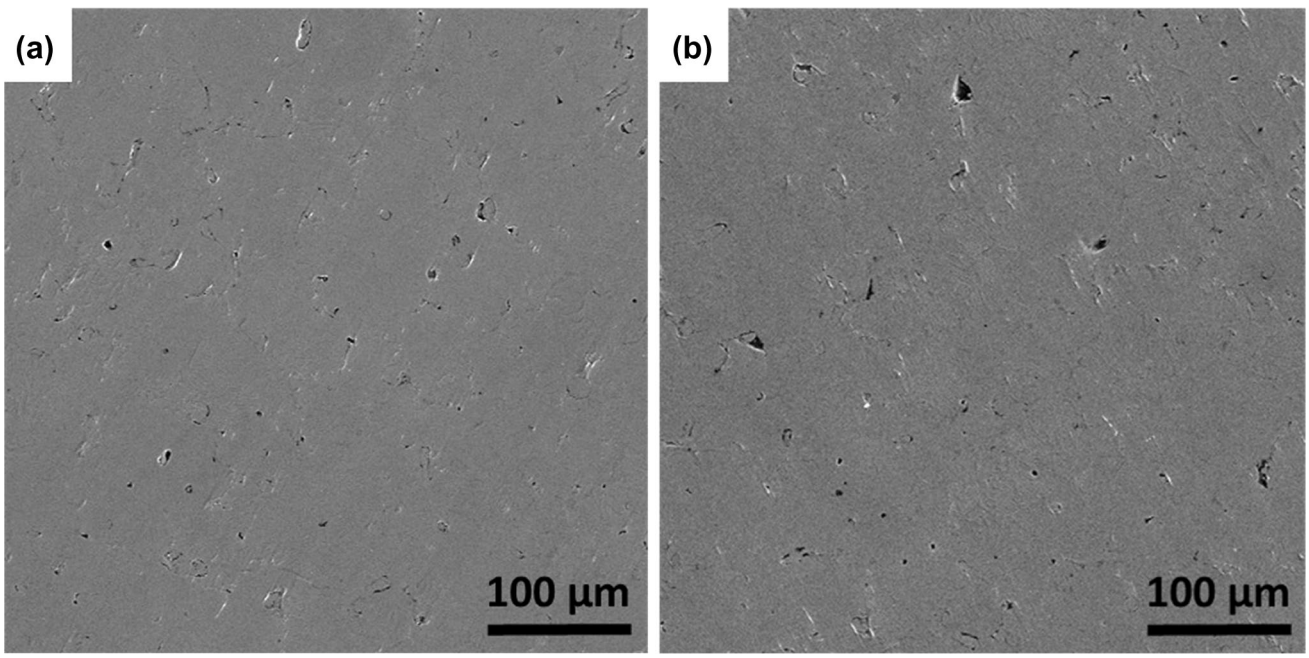

Fig. 5. SEM micrographs showing porosity distribution of parts manufactured by BJT from (a) fresh 361L powder and (b) after recycling 16 times.

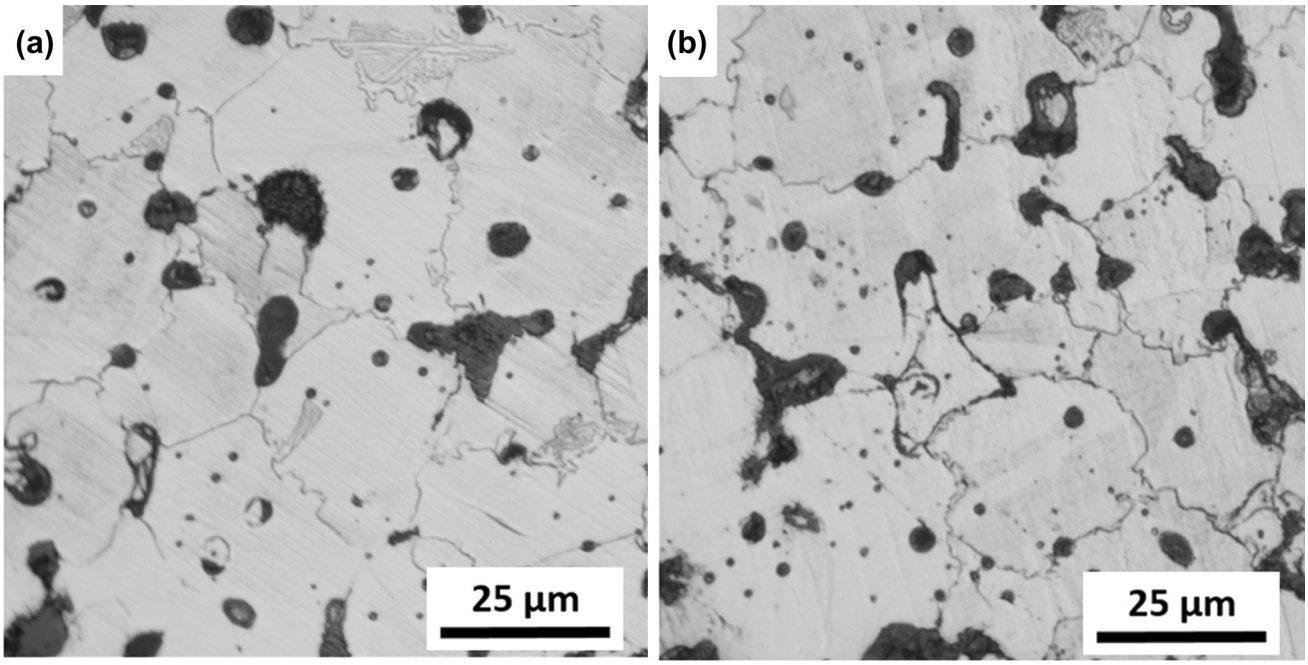

Fig. 6. Optical micrographs of parts manufactured by BJT using (a) fresh SS 316L powder, and (b) after recycling 16 times.

combined effect of the larger particle size (D_{90} = 45.10 μm) and the greater fraction of irregular-shaped particles in the recycled powder impeded good packing and spreading of the recycled powder in the bed, resulting in lower green density with larger and irregular-shaped pores. Then, during sintering, the large particle size and higher porosity led to a slower diffusion rate, resulting in the 1.5% lower density in the part manufactured from the recycled powder compared with that obtained using the fresh powder. These findings are consistent with the fundamentals of sintering. According to Herring's scaling law,[35] coarser powders need more time to achieve the same degree of sintering compared with finer particles. Similarly, at a given sintering temperature, smaller particles can achieve a higher density due to their higher surface energy.[36]

In this study, the final density of the parts manufactured by BJT using the fresh and recycled powder was 93.5 ± 0.4% and 92.0 ± 0.5%, respectively. It is noteworthy that, by optimizing the postprocessing including the sintering temperature, time, and atmosphere, the final densification of parts could be further enhanced (> 96%[37]). However, density improvement was not the primary goal of this work; instead, the relative difference between the properties of the fresh and recycled powders and the impact on the quality of the resulting parts were the main focus of this study.

Mechanical Properties of BJT Parts After Recycling

The yield strength (YS), ultimate tensile strength (UTS), and microhardness of the parts manufactured by BJT using the fresh and recycled powder are presented in Fig. 7, in comparison with casting-grade CF3M (wrought 316L according to ASTM A743), and a wrought 316L specimen, which was also measured in this study. The bars and parts produced from the parts made with fresh and recycled powder demonstrated lower tensile properties and hardness compared with conventionally manufactured 316L, possibly due to the noticeably low density of the final parts. This is because the presence of pores in the materials can significantly reduce the load-carrying area in tensile testing, leading to lower strength. Additionally, pores can be crucial sites for stress concentration and crack nucleation in tensile testing.[38,39]

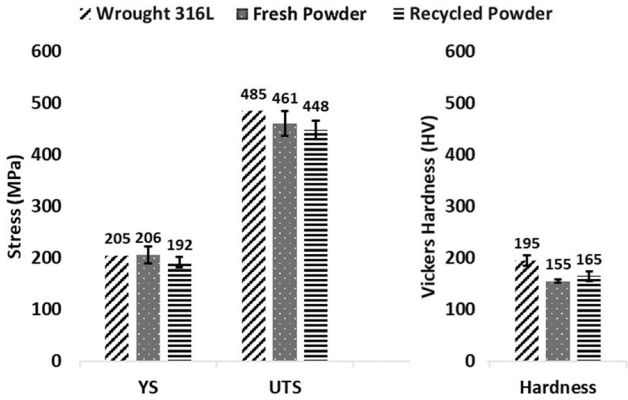

Fig. 7. Mechanical properties of wrought 316L and of parts manufactured using BJT with fresh and recycled 316L powder.

Although the microhardness of the parts manufactured using fresh and recycled powder were similar, the YS and UTS of the bars manufactured

using BJT with fresh powder were 206 ± 16 MPa and 461 ± 18 MPa, respectively, being slightly higher than when using the recycled powder with YS of 192 ± 10 MPa and UTS of 448 ± 24 MPa. The tensile properties of BJT-manufactured parts are affected by the final density, particle size, and pore size. Verlee et al.[36] reported that higher strength was achieved for SS 316L BJT sample with higher density, relatively finer particle size, and less porosity. According to Liu et al.,[32] SS 316L powder with better flowability resulted in higher UTS and hardness properties in the SLM process. In this study, the higher UTS of the parts produced using fresh powder was associated with the higher final density of the bars made from the fresh powder. Overall, despite the small differences, the mechanical properties of the parts manufactured using the fresh and recycled powder were considered to be very similar.

CONCLUSION

SS 316L powder was recycled 16 times, with each recycling step occurring after a BJT cycle. The characteristics of the powder, including the PSD and morphology, had significant effects on its packing behavior (spreadability, flowability, and green density) in the print bed, and thereby on the densification behavior and mechanical properties of the BJT parts. It was found that, despite the slight changes in the powder characteristics, the mechanical properties of the parts manufactured by BJT using the fresh and recycled powder were nearly equivalent. During recycling up to 16 times, about 4 vol.% of the processed powder was collected as waste due to agglomeration, being oversized, and possible contamination with binder, indicating an overall efficiency of material consumption of up to ~ 96%.

In investigating the effects of powder recycling on the powder characteristics and mechanical properties of the BJT-manufactured parts, the following key findings were made:

1. A trend toward coarsening of the particle size distribution was observed; the number of fine particles (< 10 μm) was reduced, whereas the number of large particles (> 30 μm) was increased, leading to higher D_{10}, D_{50}, and D_{90} values for the recycled powder due to loss of fines.
2. The flowability of recycled powder was slightly improved due to the coarsening of the particle size.
3. The adopted recycling strategy did not change the powder chemistry, except for a slight (0.036%) increase in oxygen due to oxygen pick-up from atmosphere or water-based binder.
4. The final density of parts manufactured using fresh powder was higher than when using recycled powder due to the smaller PSD and higher fraction of fine particles.
5. The tensile properties of parts manufactured by BJT from fresh and recycled powder were measured to be 206 ± 16 MPa and 461 ± 24 MPa, and 192 ± 10 MPa and 448 ± 18 MPa, respectively, due to the relatively higher final density of the parts produced using the fresh powder.

Recycling of powder in the BJT process proved to be highly efficient. However, several challenges are involved in powder recycling in BJT, for example, the presence of large powder agglomerates in the BJT-processed powder due to either binder splash or binder penetration outside the defined boundaries of the printing part. The extent of this PSD coarsening could be controlled by utilizing an effective sieving strategy. Furthermore, the adopted depowdering strategy proved to affect the morphological characteristics of the powder. Two solutions are suggested to overcome such morphological changes during depowdering: (1) utilizing soft brushes for individual depowdering of as-printed parts instead of applying pressurized air for mass depowdering of specimens. This would be a trade-off between time efficiency and quality. While the former increases the production time, the latter may be detrimental to dimensional accuracy and powder particle shape. (2) Discarding a fraction of the powder obtained from the depowdering step in the recycled powder. The material efficiency would thus be slightly reduced but the particle shape would remain unchanged.

ACKNOWLEDGEMENTS

The authors would like to acknowledge the funding of equipment provided by the Murdock Charitable Trust (Contract #2016231: MNL: 5/18/2017), Department of Energy (DOE) Advanced Manufacturing Office (AMO) and the Rapid Advancement in Process Intensification Deployment (RAPID) Institute. The authors would also like to acknowledge the research funding from the Oregon Business Development Department (OBDD), Contract #C2018121 through the High Impact Opportunity Project ("HIOP") program. The authors also thank the director and staff of the Advanced Technology and Manufacturing Institute (ATAMI) for their support. The authors would like to thank Peter Miller for conducting LECO oxygen/carbon analyses.

REFERENCES

1. B. Poorganji, E. Ott, R. Kelkar, A. Wessman, and M. Jamshidinia, *JOM* 72, 561 (2020).
2. L.C. Ardila, F. Garciandia, J.B. González-Díaz, P. Álvarez, A. Echeverria, M.M. Petite, R. Deffley, and J. Ochoa, *Phys. Procedia* 56, 99 (2014).
3. R.M. German, *Powder Metallurgy and Particulate Materials Processing: The Processes, Materials, Products, Properties, and Applications* (Princeton, NJ: Metal Powder Industries Federation Princeton, 2005).
4. A.T. Sutton, C.S. Kriewall, M.C. Leu, and J.W. Newkirk, *Virt. Phys. Prototyp.* 12, 3 (2017).

5. S. Pasebani, M. Ghayoor, S. Badwe, H. Irrinki, and S.V. Atre, *Addit. Manuf.* 22, 127 (2018).
6. M. Ghayoor, S.B. Badwe, H. Irrinki, S.V. Atre, and S. Pasebani, *Materials Science Forum*. 2018. Trans Tech Publ, vol. 941 (2018), pp. 698–703.
7. B. Utela, D. Storti, R. Anderson, and M. Ganter, *J. Manuf. Process.* 10, 96 (2008).
8. A. Mostafaei, P. Rodriguez De Vecchis, I. Nettleship, and M. Chmielus, *Mater. Des.* 162, 375 (2019).
9. A.-B. Yu, J. Bridgwater, and A. Burbidge, *Powder Technol.* 92, 185 (1997).
10. A.B. Spierings and G. Levy. in *Proceedings of the Annual International Solid Freeform Fabrication Symposium*. 2009. Austin, TX.
11. S. Mirzababaei and S. Pasebani, *J. Manuf. Mater. Process.* 3, 82 (2019).
12. H.G. Coe and S. Pasebani, *J. Manuf. Mater. Process.* 4, 8 (2020).
13. R. O'Leary, R. Setchi, P. Prickett, and G. Hankins, *InImpact. J. Innov. Impact* 8, 377 (2016).
14. V. Seyda, N. Kaufmann, and C. Emmelmann, *Phys. Procedia* 39, 425 (2012).
15. A. Strondl, O. Lyckfeldt, H. Brodin, and U. Ackelid, *JOM* 67, 549 (2015).
16. P. Nandwana, W.H. Peter, R.R. Dehoff, L.E. Lowe, M.M. Kirka, F. Medina, and S.S. Babu, *Metall. Mater. Trans. B* 47, 754 (2016).
17. G. Jacob, G. Jacob, C.U. Brown, M.A. Donmez, S.S. Watson, and J. Slotwinski, *Effects of Powder Recycling on Stainless Steel Powder and Built Material Properties in Metal Powder Bed Fusion Processes* (Gaithersburg, MD: US Department of Commerce, National Institute of Standards and Technology, 2017).
18. H. Miyanaji, N. Momenzadeh, and L. Yang, *Addit. Manuf.* 20, 1 (2018).
19. N.D. Parab, J.E. Barnes, C. Zhao, R.W. Cunningham, K. Fezzaa, A.D. Rollett, and T. Sun, *Sci. Rep.* 9, 1 (2019).
20. ASTM, *Standard Specification for Additive Manufacturing Stainless Steel Alloy (UNS S31603) with Powder Bed Fusion*. 2016.
21. M. Lutter-Günther, C. Gebbe, T. Kamps, C. Seidel, and G. Reinhart, *Prod. Eng.* 12, 377 (2018).
22. R. Grey and J. Beddow, *Powder Technol.* 2, 323 (1969).
23. K. Lu, M. Hiser, and W. Wu, *Powder Technol.* 192, 178 (2009).
24. D. Schulze, *Behaviour, Characterization, Storage and Flow* (Berlin: Springer, 2008), p. 22.
25. A. Butscher, M. Bohner, C. Roth, A. Ernstberger, R. Heuberger, N. Doebelin, P.R. Von Rohr, and R. Müller, *Acta Biomater.* 8, 373 (2012).
26. P.R. Baker, *Three Dimensional Printing with Fine Metal Powders* (Cambridge, MA: Massachusetts Institute of Technology, 1997).
27. Y. Zhang, E. Feng, W. Mo, Y. Lv, R. Ma, S. Ye, X. Wang, and P. Yu, *Metals* 8, 893 (2018).
28. P. Suri, R.P. Koseski, and R.M. German, *Mater. Sci. Eng. A* 402, 341 (2005).
29. A. Ramirez and J. Lippold, *Mater. Sci. Eng. A* 380, 245 (2004).
30. M. Ghayoor, S. Mirzababaei, K. Lee, Y. He, C.-h. Chang, B. K. Paul, and S. Pasebani. in *Annual International Solid Freeform Fabrication Symposium: Austin, TX, USA*. 2019.
31. D. Bourell, B. Stucker, A. Spierings, N. Herres, and G. Levy, *Rapid Prototyp. J.* 17, 195 (2011).
32. B. Liu, R. Wildman, C. Tuck, I. Ashcroft, and R. Hague, Additive manufacturing research group, Loughborough University, pp. 227–238 (2011).
33. M. Turker, D. Godlinski, and F. Petzoldt, *Mater. Charact.* 59, 1728 (2008).
34. Z. Zhou, F. Buchanan, C. Mitchell, and N. Dunne, *Mater. Sci. Eng. C* 38, 1 (2014).
35. C. Herring, *J. Appl. Phys.* 21, 301 (1950).
36. B. Verlee, T. Dormal, and J. Lecomte-Beckers, *Powder Metall.* 55, 260 (2012).
37. R. Frykholm, Y. Takeda, B.-G. Andersson, and R. Carlström, *J. Jpn. Soc. Powder Powder Metall.* 63, 421 (2016).
38. R. Rice, *J. Mater. Sci.* 28, 2187 (1993).
39. M. Jia, D. Zhang, J. Liang, and B. Gabbitas, *Metall. Mater. Trans. A* 48, 2015 (2017).